

Radiative parton energy loss and baryon stopping in AA collisions

B.G. Zakharov

L.D. Landau Institute for Theoretical Physics, GSP-1, 117940, Kosygina Str. 2, 117334 Moscow, Russia

(Dated: August 13, 2019)

We study the radiative energy loss contribution to proton stopping in AA collisions. The analyses is performed within the light-cone path integral approach to induced gluon emission. We have found that the radiative correction can fill in partly the midrapidity dip in the net proton rapidity distribution in AA collisions at $\sqrt{s} \sim 10$ GeV. We argue that at $\sqrt{s} \sim 10$ GeV the net proton fluctuations at midrapidity may be dominated by the initial fluctuations of the proton flow, which, to a good accuracy, should be binomial.

1. The baryon stopping in hadron and nucleus collisions has attracted much attention for a long time. But up to now, there is no consensus yet on the mechanism of the baryon number transfer over a large rapidity interval (which is also closely related to the mechanism of $B\bar{B}$ -annihilation). Presently, there is no answer to the most basic question about the baryon production: whether the baryon number carriers are quarks. It was proposed long ago [1] that a purely gluonic object—the so-called string junction (SJ) may play role of the baryon number carrier. In [1] it was suggested to describe the processes with baryons in the topological expansion (TE) scheme [2, 3] by treating the baryon as a Y shaped string configuration with the SJ. In this picture the baryon number transfer is associated with the transfer of the SJ. Say, $B\bar{B}$ annihilation corresponds to SJ- $\bar{S}\bar{J}$ annihilation.

In the standard quark-gluon string model QGSM [4–6], based on the TE scheme [2], it is assumed that the baryon can be treated as a quark-diquark system with a point like diquark in the $\{\bar{3}\}$ color state. From the point of view of the SJ picture [1], it means that the SJ belongs to diquark (we denote this mechanism by D-SJ). In this approximation diquarks/antidiquarks are playing the role of the baryon number carriers in processes with baryons. In the QGSM the net proton ($\Delta p = p - \bar{p}$) midrapidity density in pp collisions is related to the diquark distribution in the proton at small fractional momentum x , where it is $\propto x^{\alpha_R(0) - 2\alpha_N(0)}$ with $\alpha_R(0) \approx 0.5$ and $\alpha_N(0) \approx -0.5$ intercepts of the meson and nucleon Regge trajectories [7]. This leads to the energy dependence of the net proton midrapidity density $dN_{\Delta p}/dy \propto 1/s^{2.25}$. This disagrees strongly with the experimentally observed at ISR energies [8] s -dependence $dN_{\Delta p}/dy \propto 1/s^n$ with $n \approx 0.25$. The model with the diquarks in the antitriplet color state also underestimates the midrapidity net baryon production in AA collisions [9, 10].

In [11] it was proposed that the baryon number transfer over a large rapidity interval can be related to breaking of the antitriplet diquark due to its transition from $\{\bar{3}\}$ to $\{6\}$ color state after one gluon t -channel exchange. The transition $D_{\{\bar{3}\}} \rightarrow D_{\{6\}}$ should lead to creation of the string configuration with the SJ located near the valence quark (we denote this mechanism as q-SJ). Hadronization of such string configurations leads naturally to the energy dependence of the midrapidity net proton density $dN/dy \propto 1/s^{\alpha_R(0)/2}$ which agrees with the data. Contribution of the q-SJ mechanism of the baryon number transfer over a large rapidity interval should be enhanced in AA collisions due to increase of the probability of the $D_{\{\bar{3}\}} \rightarrow D_{\{6\}}$ transition in the nuclear matter. Similarly to pp collisions, in AA collisions the diquark breaking leads to the net proton midrapidity distribution $\propto 1/s^{\alpha_R(0)/2}$ [12].

The contribution from the q-SJ mechanism to the net proton midrapidity density in AA collisions becomes of the order of that from the ordinary D-SJ mechanism at $\sqrt{s} \sim 20$ GeV. At energies $\sqrt{s} \sim 10$ GeV contribution of the q-SJ mechanism is relatively small. One more effect of the nuclear matter that can increase the baryon number flow to the midrapidity, which can potentially be important at $\sqrt{s} \lesssim 10$ GeV, is the diquark radiative energy loss. At high energies the radiative energy loss (which is not very large) cannot increase considerably the contribution of the D-SJ mechanism, and the radiative correction to the D-SJ mechanism cannot compete with the q-SJ mechanism. But at $\sqrt{s} \lesssim 10$ GeV, where the contribution of the q-SJ mechanism becomes small, the radiative mechanism might be important, and it is of great interest to understand how large the radiative contribution to the baryon stopping can be.

The question of how the baryon number flows to the midrapidity, which is interesting in itself, at energies $\sqrt{s} \lesssim 10$ GeV is also of great importance in connection with the future experiments at NICA and the beam energy scan (BES) program at RHIC aimed to search for the QCD critical point. One of the important signals of the critical point may be the non-monotonic variation of the moments of the net-baryon distribution in the central rapidity region [13]. However, in the event-by-event fluctuations of the net-baryon yield a considerable contribution may come from the initial state fluctuations [14]. One can expect that, similarly to the situation with the baryon number fluctuations in the QGP and the hadron gas [14, 15], for the D-SJ mechanism the variance for the net-baryon number should be bigger by a factor of ~ 3 than in the picture with the baryon number associated with quarks.

In the present paper we calculate the the diquark and quark radiative energy loss in AA collisions within the light-cone path integral (LCPI) approach [16–18] to the induced gluon emission. We study the effect of the diquark radiative

energy loss in the nuclear matter on the net proton rapidity distribution for the D-SJ mechanism. We perform comparison with the data on the proton distribution in Pb+Pb collisions at $\sqrt{s} = 8.76$ GeV from NA49 Collaboration [19].

2. The scalar ud diquark, which dominates in the nucleon wave function [20–22], is a rather compact object. It has a formfactor $F(Q^2) \approx 1/[1 + Q^2/Q_0^2]$ with $Q_0^2 \approx 10$ GeV² [20]. The typical virtuality scale for the induced gluon emission in the nuclear matter ($\sim m_g^2 \lesssim 0.5$ GeV²) is much smaller than Q_0^2 . For this reason the induced gluon radiation from scalar diquarks can be calculated as for a point like particle. This approximation should be reasonable even for the less compact vector ud and uu diquarks, for which $Q_0^2 \approx 2$ GeV² [20].

We will treat nuclei as uniform spheres. We consider AA collisions in the rest frame of one (target) of the colliding nuclei. To a good approximation, the induced gluon emission from each diquark/quark in the projectile nucleus can be evaluated similarly to pA collisions, i.e. ignoring the presence of other nucleons. Indeed, the typical transverse size for the induced gluon emission is $\sim 1/m_g$. The typical number of nucleons in the tube of radius $r \sim 1/m_g$ in the projectile nucleus is $\mu \sim A/R_A^2 m_g^2$. For $m_g \sim 400 - 800$ MeV it gives $\mu \sim 0.4 - 1.5$ for heavy nuclei with $A \sim 200$. This estimate shows that the possible collective effects in the projectile nucleus should not be strong.

In the LCPI approach the x -spectrum of the induced $a \rightarrow bc$ transition in the fractional longitudinal momentum $x = x_b = E_b/E_a$ can be written as (we take the z -axis along the projectile momentum) [16, 18]

$$\frac{dP}{dx} = 2\text{Re} \int_{-\infty}^{\infty} dz_1 \int_{z_1}^{\infty} dz_2 \exp[-i(z_2 - z_1)/L_f] \hat{g} [\mathcal{K}(\boldsymbol{\rho}_2, z_2 | \boldsymbol{\rho}_1, z_1) - \mathcal{K}_0(\boldsymbol{\rho}_2, z_2 | \boldsymbol{\rho}_1, z_1)] \Big|_{\boldsymbol{\rho}_{1,2}=0}. \quad (1)$$

Here \mathcal{K} is the Green's function for the Schrödinger equation with the Hamiltonian

$$H = -\frac{1}{2M} \left(\frac{\partial}{\partial \boldsymbol{\rho}} \right)^2 + v(\boldsymbol{\rho}, z), \quad (2)$$

$$v(\boldsymbol{\rho}, z) = -i \frac{n(z) \sigma_3(\boldsymbol{\rho}, x)}{2}, \quad (3)$$

where $M(x) = E_a x(1-x)$, $L_f = 2M/[m_b^2 x_c + m_c^2 x_b - m_a^2 x_b x_c]$, n is the medium density, and $\sigma_3(\boldsymbol{\rho}, x)$ is the cross section of interaction of the $bc\bar{a}$ system with a nucleon, \mathcal{K}_0 is the vacuum Green's function for $v = 0$. \hat{g} is the vertex factor given by

$$\hat{g} = \frac{\alpha_s P_{ba}}{2M^2} \cdot \frac{\partial}{\partial \boldsymbol{\rho}_1} \cdot \frac{\partial}{\partial \boldsymbol{\rho}_2}, \quad (4)$$

where P_{ba} is ordinary splitting function (for $q \rightarrow gq$ $P_{gq} = C_F[1 + (1-x)^2]/x$, and for $D \rightarrow gD$ $P_{gD} = 2C_F(1-x)/x$). The three-body cross section, entering the imaginary potential (3), for the $D(q) \rightarrow gD(q)$ processes can be expressed in terms of the dipole cross section for the color singlet $q\bar{q}$ pair [23]

$$\sigma_3(\boldsymbol{\rho}, x) = \frac{9}{8} [\sigma_2(\boldsymbol{\rho}) + \sigma_2((1-x)\boldsymbol{\rho})] - \frac{1}{8} \sigma_2(x\rho). \quad (5)$$

In the limit of $L_f \gg L$ the radiation rate is dominated by the configurations with large negative z_1 and large positive z_2 $|z_{1,2}| \gg L$ (L is thickness of the target, for a nucleus with radius R_A $\langle L \rangle \approx 4R_A/3$). In this regime the spectrum (1) may be calculated treating the transverse parton positions during traversing the target as frozen. The integrals over $z_{1,2}$ outside the target region on the right hand side of (1) can be expressed via the vacuum light-cone wave function for the $a \rightarrow bc$ [18], and the Green' function in the medium is reduced to the ordinary Glauber attenuation factor for the $bc\bar{a}$ system. This leads to the formula [18, 24]

$$\frac{dP_{fr}}{dx} = 2 \int d\boldsymbol{\rho} |\Psi(x, \boldsymbol{\rho})|^2 \left\{ 1 - \exp \left[-\frac{nL\sigma_3(\boldsymbol{\rho}, x)}{2} \right] \right\}, \quad (6)$$

where Ψ is the light-cone wave function of the bc system in the $(x, \boldsymbol{\rho})$ representation. The frozen-size approximation is widely used in physics of AA collisions, e.g., it was used for evaluation of the gluon spectrum in [25]. This approximation should be good for emission of gluons with energies $\omega \gg 10 - 20$ GeV (in the target nucleus rest frame). But for AA collision at $\sqrt{s} \sim 10$ GeV, interesting to us here, the typical gluon energies turn out to not big enough for its applicability.

We will perform calculation for the quadratic approximation $\sigma_{q\bar{q}}(\boldsymbol{\rho}) = C_2 \rho^2$ (C_2 may be written in terms of the well known transport coefficient \hat{q} [26] as $C_2 = \hat{q} C_F / 2n C_A$). In this case the Hamiltonian (2) in the medium takes an

oscillator form with the complex frequency given by $\Omega = \sqrt{-inC_3/M}$ with $C_3 = C_2\{\frac{9}{8}[1 + (1-x)^2] - \frac{x^2}{8}\}$. In the oscillator approximation the Green's function can be written in the form

$$\mathcal{K}(\boldsymbol{\rho}_2, z_2 | \boldsymbol{\rho}_1, z_1) = \frac{\gamma}{2\pi i} \exp [i(\alpha \boldsymbol{\rho}_2^2 + \beta \boldsymbol{\rho}_1^2 - \gamma \boldsymbol{\rho}_1 \cdot \boldsymbol{\rho}_2)]. \quad (7)$$

Only the parameter γ is important in calculating the x -spectrum. From (1), (7) one can obtain

$$\frac{dP}{dx} = \frac{\alpha_s P_{ba}(x)}{\pi M^2} \text{Re} \int_{-\infty}^{\infty} dz_1 \int_{z_1}^{\infty} dz_2 \exp [-i(\xi_2 - \xi_1)/L_f] \cdot (\gamma_0^2 - \gamma^2). \quad (8)$$

Here $\gamma_0 = M/(z_2 - z_1)$ is the parameter γ in (7) for vacuum when $\Omega = 0$, and

$$\gamma = M\Omega \times \begin{cases} \sin^{-1}(\Omega(z_2 - z_1)) & \text{at } L > z_2 > z_1 > 0, \\ \{\cos(\Omega(L - z_1)) \cdot [\tan(\Omega(L - z_1)) + \Omega(z_2 - L)]\}^{-1} & \text{at } z_2 > L > z_1 > 0, \\ \{\cos(\Omega z_2) \cdot [\tan(\Omega z_2) + \Omega|z_1|]\}^{-1} & \text{at } L > z_2 > 0 > z_1, \\ \{\cos(\Omega L) \cdot [\Omega(z_2 - z_1 - L) + \tan(\Omega L)(1 - \Omega^2(z_2 - L)|z_1|)]\}^{-1} & \text{at } z_2 > L, z_1 < 0. \end{cases} \quad (9)$$

3. For numerical calculations we take $\alpha_s = 0.5$. We use the value $\hat{q} = 0.01 \text{ GeV}^3$, supported by calculations of the coefficient C_2 using the double gluon formula for the dipole cross section [17]. For the quark and diquark masses we take $m_q = m_D = 300 \text{ MeV}$. However, the radiative energy loss is only weakly dependent on the specific choice of the mass of the initial fast particle. But its dependence on the gluon mass, which plays the role of the infrared cutoff, turns out to be rather strong¹. We perform numerical computations for $m_g = 750 \text{ MeV}$ and $m_g = 400 \text{ MeV}$. The former value was obtained in the analysis within the dipole BFKL equation [28] of the data on the low- x proton structure function F_2 . The values of m_g in the range 400 – 800 MeV have been predicted in the nonperturbative calculations using the Dyson-Schwinger equations [29–31]. We take for Pb nucleus $R_A = 6.49 \text{ fm}$, that corresponds to the typical parton path length in the nuclear matter $\langle L \rangle \approx 8.65 \text{ fm}$.

In Fig. 1 we present the result for the total radiative energy loss for diquarks and quarks for Pb nucleus

$$\Delta E = E \int_{x_{min}}^{x_{max}} dx x \frac{dP}{dx}. \quad (10)$$

We take $x_{min} = m_g/E$ and $x_{max} = 1 - m_q/E$. To illustrate the effect of the parton transverse motion we show in Fig. 1 also the prediction obtained with the spectrum calculated in the frozen-size approximation (6). One can see that the frozen-size approximation underestimates the energy loss by a factor of 1.6 – 1.7 (1.2 – 1.3) at $m_g = 400(750) \text{ MeV}$. Thus, the frozen-size approximation turns out to be rather crude. Fig. 1 shows that the ratio $\Delta E/E$ flatten at $E \gtrsim 50 - 100 \text{ GeV}$, and at $E \sim 1000 \text{ GeV}$ for diquark $\Delta E/E \approx 0.18(0.062)$ at $m_g = 400(750) \text{ MeV}$. Note that some violation of the $1/m_g^2$ scaling for ΔE is due to the Landau-Pomeranchuk-Migdal suppression that is stronger for smaller m_g .

For evaluation of the net baryon spectrum within the QGSM one needs only the contribution of the diquark fragmentations to baryons, i.e. the contribution from color strings with the valence diquarks. In pp and AA collisions the contributions from the projectile nucleons (diquark-quark strings) and from the target nucleons (quark-diquarks strings) can be evaluated independently. The valence quarks and sea quarks/diquarks are irrelevant. The net baryon x -distribution for each projectile nucleon in the QGSM can be written as [9, 10]

$$\frac{dN_{AA}^{\Delta B}}{dx} \approx \int_x^1 \frac{dz}{z} \rho_D(z) D_D^B(x/z), \quad (11)$$

¹ Note the the situation with the infrared sensitivity of the radiative energy loss for a parton incident on the medium from outside is very different from that for a parton produced inside the medium. In the former case the fast parton approaches the target with a formed gluon cloud with the transverse size $\sim 1/m_g$. While in the latter case the fast parton is produced without the formed gluon cloud. After gluon emission the transverse size of the two-parton system grows $\propto \sqrt{L/\omega}$ [27]. As a result for gluons with $L_f \gtrsim L$ the spectrum depends weakly on the gluon mass. This leads to a weak infrared sensitivity of the total parton energy loss [27].

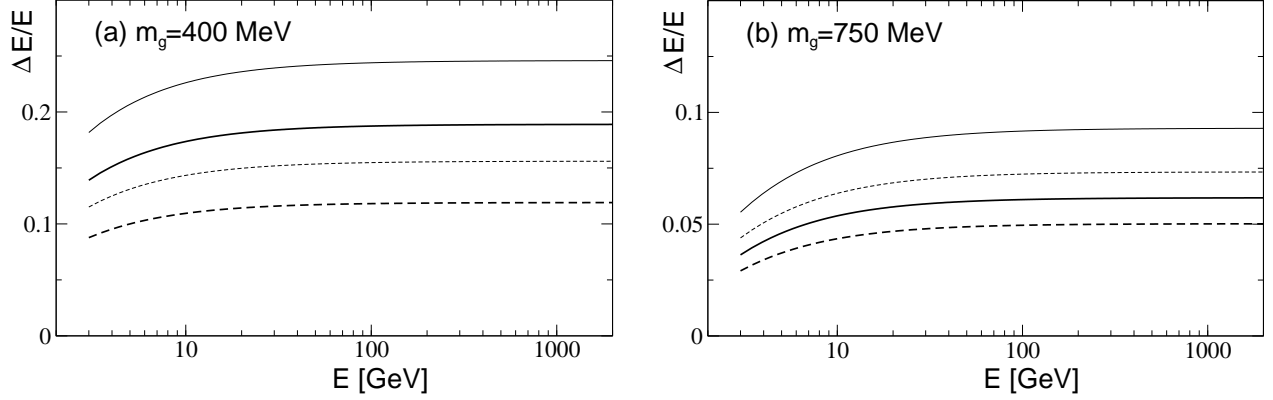


FIG. 1: The fractional diquark (thick solid) and quark (thin solid) radiative energy loss versus energy for Pb nucleus obtained using (10) with accurate gluon spectrum (8) for (a) $m_g = 400$ MeV and (b) $m_g = 750$ MeV. The dashed line shows same for gluon spectrum calculated in the frozen-size approximation (6).

where ρ_D is the diquark distribution in the projectile nucleon, D_D^B is the $D \rightarrow B$ fragmentation function. We use for the diquark distribution the parametrization of the form used in the [9, 10]

$$\rho_D(x) = C x^{\alpha_R(0) - 2\alpha_N(0)} (1-x)^{-\alpha_R(0) - 1 + k}, \quad (12)$$

where $C = [\int_0^1 dx \rho_D(x)]^{-1}$ is the normalization constant. The parameter k controls the energy degradation due to creation of additional sea $q\bar{q}$ pairs in the nucleon, that lead to formation of additional color strings in the final state. Within the QGSM there is no a rigorous theoretical method for its determination. It is input by hand in order to reproduce experimental data. In the case of pp collisions data on the charged particle multiplicities can be reasonably described using the quasicone formulas [32]. However, the model fails to describe the AA data [32]. In [9, 10, 12] the value of k was set to $\nu = 2N_{col}/N_{part}$ (here N_{col} and N_{part} are the number of the binary collisions and the number of participant nucleons evaluated in the Glauber model). In terms of the wounded nucleon model [33, 34] ν is simply the average number of inelastic collisions per participant nucleon. This prescription gives reasonable agreement with the data on charged particle multiplicity in AA collisions [9]. In the present analysis we use a slightly modified formula $k = \nu + \langle k_N \rangle - 1$, where $\langle k_N \rangle$ is the average number of cut Pomerons in the quasicone formulas for pp collisions ($\langle k_N \rangle \approx 1.65$ at $E = 40$ GeV). This modification practically does not change the charged particle multiplicity for AA collisions, but it somewhat improves description of the data on the baryon stopping in pp and AA collisions. Also, this prescription ensures matching of the predictions for very peripheral AA collisions with that for pp collisions.

The induced gluon emission in AA collisions softens the diquark and quark distributions due to the radiative energy shift. However, if one neglects the diquark transitions to the $\{6\}$ color state, the radiative change of the quark distribution is irrelevant for the baryon stopping. But the radiative diquark energy loss should increase the baryon stopping as compared to the predictions of the QGSM. In the presence of the induced gluon emission we write the diquark distribution as (we denote it by ρ_D^{eff})

$$\rho_D^{eff}(x) = \rho_D(x) + \Delta\rho_D(x), \quad (13)$$

where $\Delta\rho_D(x)$ is the radiative correction. In terms of the induced gluon spectrum (1), the radiative correction to the QGSM diquark distribution ρ_D can be written as

$$\Delta\rho_D(x) = \int_{x_{min}}^{1-x} dz \frac{dP}{dz} \left[\frac{\rho_D(x/(1-z))}{1-z} - \rho_D(x) \right]. \quad (14)$$

Here the second term in the square brackets is due to reduction of the probability to find the diquark without gluon emission. Note that due to this term the radiative softening of the diquark distribution is insensitive to the z -dependence of the gluon spectrum at $z \rightarrow 0$.

In Fig. 2a we confront the results of our calculations with and without the induced gluon emission of the net proton rapidity spectrum (in the center of mass frame) with the data from NA49 Collaboration for Pb+Pb collisions at $E = 40$ GeV ($\sqrt{s} = 8.76$ GeV) [19]. The theoretical curves are obtained by summing the contributions of the valence proton flow from the projectile and the target nuclei. The calculations are performed with the fragmentation function $D \rightarrow p$ from [35] $D_D^p(z) = az^{1.5}$. The value of the normalization parameter a depends on the strange suppression

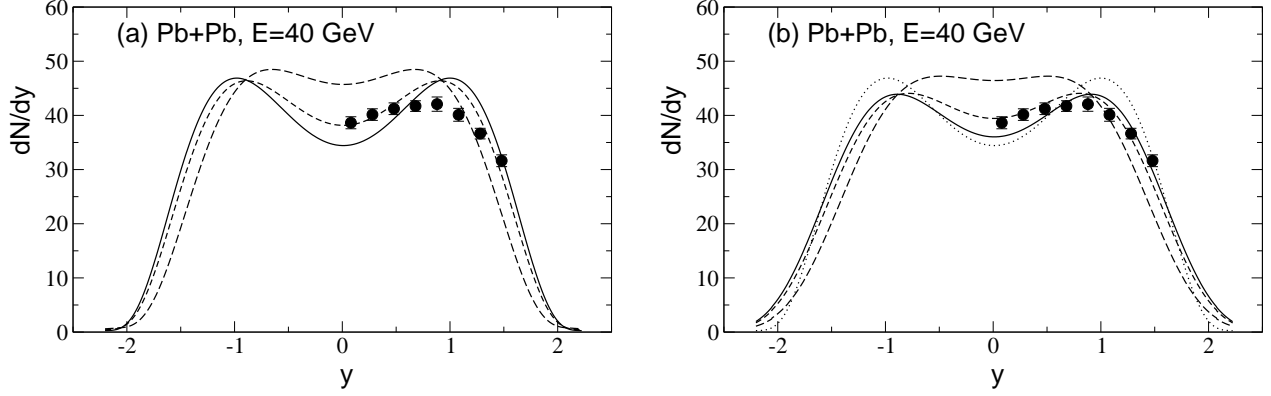


FIG. 2: (a) The net proton rapidity distribution in 0 – 5% central Pb+Pb collisions at $E = 40$ GeV obtained without (solid) and with the radiative correction for $m_g = 400$ MeV (long dashes) and for $m_g = 750$ MeV (short dashes). Data points are from NA49 [19]. (b) Same as (a) accounting for the Gaussian smearing with the diffusion width $\sigma_d = 0.3$, the dotted line shows the distribution without radiative and diffusion corrections (same as solid line in the left panel).

factor S/L ($2L + S = 1$) introduced in [35], for which we take $S/L = 0.367$. This value was adjusted to reproduce the experimental midrapidity ratio $p/\Lambda \approx 0.4$ for Pb+Pb collisions at $E = 40$ GeV [19, 36]. From Fig. 2a one sees that the radiative correction partly fills in the minimum at $y = 0$. It increases the spectrum at $y = 0$ by a factor of about 1.35 and 1.12 for $m_g = 400$ and 750 MeV, respectively. Thus, we conclude that for $m_g = 750$ MeV the radiative effect is relatively weak. For $m_g = 400$ MeV the radiative effect is quite strong, and the theoretical spectrum overshoot the data at $y \sim 0$. Of course, one can improve agreement with the data by changing the QGSM parton distributions, which have not stringent theoretical constraints in the QGSM. However, in this preliminary study our purpose is to understand if the radiative energy loss may be important, and not as good as possible fitting to the data.

Our results shown in Fig. 2a do not include the possible baryon diffusion in the hot QCD matter produced after interaction of the colliding nuclei at the proper time $\tau_0 \approx 2R_A/\gamma$ (γ is the nucleus Lorentz factor in the center of mass frame). For $E = 40$ GeV ($\gamma \approx 4.7$) we have $\tau_0 \approx 2.8$ fm. The change of the baryon rapidity is related to its random walk in the longitudinal z direction in the comoving frame of the QCD matter. For the diffusion mean squared rapidity fluctuations one can easily obtain

$$\langle \Delta y_d(\tau)^2 \rangle^{1/2} \approx \int_{\tau_0}^{\tau} \frac{\langle \Delta z(\tau)^2 \rangle^{1/2}}{d\tau} \frac{d\tau}{\tau}. \quad (15)$$

Making use of the random walk formula $\langle \Delta z(\tau)^2 \rangle = (\tau - \tau_0) \bar{v} l_c / 3$ (here \bar{v} is the mean proton velocity, l_c is the proton mean free path length) from (15) one obtains

$$\langle \Delta y_d(\tau)^2 \rangle^{1/2} \approx \sqrt{\frac{\bar{v} l_c}{3\tau_0}} \left[\frac{\pi}{2} - \arcsin \left(\sqrt{\tau_0/\tau_f} \right) \right], \quad (16)$$

where τ_f is the freeze out proper time. From the relation for the initial entropy density $s_0 = \frac{C}{\tau_0 \pi R_A^2} \frac{dN_{ch}}{d\eta}$ ($C = dS/dy / dN_{ch}/d\eta \approx 7.67$ is the entropy/multiplicity ratio [37]), using the midrapidity charged particle density $dN_{ch}/d\eta \approx 280$ [19, 38] and the lattice QCD matter EoS [39] we obtain $T_0 \approx 170 - 175$ MeV for $\tau_0 \approx 2.8$ fm. Using the hadron gas model for the relevant range of the temperature $T \sim 140 - 175$ MeV from (16) with $\tau_f \approx 13$ fm [40] one obtains $\langle \Delta y_d(\tau_f)^2 \rangle^{1/2} \approx 0.3$. To illustrate the magnitude of the diffusion correction, in Fig. 2b we show the prediction obtained with the Gaussian smearing with the width $\sigma_d = 0.3$. One sees that the smearing partly fills in the minimum.

From Figs. 2a, b one can see that the diffusion effect should not affect strongly the net proton rapidity distribution. However, one can expect that for $\sigma_d \sim 0.3$ the diffusion may be important for the event-by-event net proton fluctuations for the rapidity window Δy about $\sim 2 - 3$ units of σ_d . In this regime the diffusion can modify somewhat the primordial net proton yield fluctuations. But, at the same time, it is clear that for $\Delta y/\sigma_d \sim 3$ this modification cannot be strong. For this reason the net baryon charge fluctuations cannot be described by the grand canonical ensemble formulas which require $\sigma_d \gg \Delta y$, and one cannot expect to observe a real critical regime. In the light of this, the absence of a clear signal of the critical point in the net proton fluctuations at $\sqrt{s} \sim 10$ GeV for $|y| < 0.5$ in Au+Au collisions from STAR [41] is not surprising. For the diquark mechanism of the baryon flow, to a good accuracy, these fluctuations should be

binomial. This agrees with the STAR observation [41] that the net proton fluctuations are close to binomial/Poissonian at $\sqrt{s} \sim 10$ GeV, where the antiproton yield becomes very small. In the scenario of [42], in which the carriers of baryon number are quarks, the binomial/Poissonian distribution occurs for the net quark fluctuations. In this case $\langle (N_{\Delta p} - \langle N_{\Delta p} \rangle)^2 \rangle \approx \langle N_{\Delta p} \rangle / 3$ (cf. [15]), which contradicts the STAR measurement [41]. Note that even without calculating the diffusion width σ_d , the existence of the dip in the experimental net proton distribution at $y = 0$ from NA49 [19] says that σ_d is considerably smaller than ~ 1 . Because, numerical calculations show that for $\sigma_d \sim 1$ the diffusion should completely wash out the dip. So, one can say, that we have an experimental evidence that at $\sqrt{s} \sim 10$ GeV the net proton fluctuations for $\Delta y \sim 1$ cannot not be close the critical point regime.

One remark is in order regarding the status of the parton radiative energy loss in the nuclear matter in the string model. One might wonder whether the adding of the radiative energy loss leads to the double counting, because the QGSM already includes the energy degradation of the ends of the strings for multiple Pomeron exchanges. However, in the TE/QGSM the energy degradation is due to creation of the parallel hadronic states, say, $h_1 \rightarrow h_2 h_3$ for two Pomeron exchanges. In the TE [2], based on the $1/N$ expansion ($N = N_c$, $N_F/N_c = \text{const}$), such parallel energy degradation is due to the quark loops that survive at $N \rightarrow \infty$, only because $N_F \rightarrow \infty$ together with N_c . On the contrary, the induced gluon emission is a purely gluonic effect, which does not depend on N_F at all. Contrary to the parallel energy degradation in the TE, this mechanism does not increase the number of the color strings (as in the LUND model [43] the radiated gluon may be treated as a kink on the available string attached to the diquark). Thus, it is clear the radiative mechanism is absent in the ordinary QGSM [4–6]. From the point of view of the TE it is a subleading (in $1/N$) effect. Our calculations show that its contribution to the midrapidity net proton density at $\sqrt{s} \sim 10$ GeV may be quite large.

4. In summary, we have studied, for the first time, the radiative energy loss contribution to the proton stopping in AA collisions in the energy region $\sqrt{s} \sim 10$ GeV which is of interest in connection with the future experiments at NICA and the BES program at RHIC. The analyses is based on the LCPI approach [16, 17] to the induced gluon emission. Calculation are performed beyond the soft gluon approximation. We have compared our results with the data on the proton rapidity distribution from NA49 [19] for central Pb+Pb collisions at $E = 40$ GeV. We have found that the radiative correction can fill in partly the midrapidity dip in the net proton rapidity distribution. For $m_g \sim 400$ MeV the radiative effect turns out to be rather strong, and its contribution to the midrapidity net proton density is comparable to the prediction of the ordinary QGSM.

We argue that the net proton midrapidity fluctuations at $\sqrt{s} \sim 10$ GeV may be dominated by the initial fluctuations of the proton flow to the midrapidity region. The fact the net proton distribution from STAR [41] at $\sqrt{s} \sim 10$ GeV is close to the Poissonian/binominal distribution provides evidence for the diquark mechanism of the baryon flow, while disfavors the picture where quarks (without SJ) transmit the baryon number [42]. The dominance of the initial state fluctuations makes questionable observation of the QCD critical point via the data on the net proton fluctuations in a rapidity window $\Delta y \sim 1$.

This work was partly supported by the RFBR grant 18-02-40069mega.

-
- [1] G.C. Rossi and G. Veneziano, Nucl. Phys. B**123**, 507 (1977).
 - [2] G. Veneziano, Phys. Lett. B**52**, 220 (1974).
 - [3] G. Veneziano, Nucl.Phys. B**117**, 519 (1976).
 - [4] G. Cohen-Tannoudji, A.E. Hassouni, J. Kalinowski, and R.B. Peschanski, Phys. Rev. D**19**, 3397 (1979).
 - [5] A. Capella and J. Tran Thanh Van, Phys. Lett. B**114**, 450 (1982).
 - [6] A.B. Kaidalov, Phys. Lett. B**116**, 459 (1982).
 - [7] A.B. Kaidalov and O.I. Piskunova, Z. Phys. C**30**, 145 (1986).
 - [8] B. Alper *et al.*, Nucl. Phys. B**100**, 237 (1975).
 - [9] A. Capella, A. Kaidalov, A.K. Akil, C. Merino, and J. Tran Thanh Van, Z. Phys. C**70**, 507 (1996) [hep-ph/9507250].
 - [10] A. Capella and C.A. Salgado, Phys. Rev. C**60**, 054906 (1999) [hep-ph/9903414].
 - [11] B.Z. Kopeliovich and B.G. Zakharov, Z. Phys. C**43**, 241 (1989).
 - [12] A. Capella and B.Z. Kopeliovich, Phys. Lett. B**381**, 325 (1996) [hep-ph/9603279].
 - [13] M.A. Stephanov, Phys. Rev. Lett. **102**, 032301 (2009) [arXiv:0809.3450].
 - [14] M. Asakawa and M. Kitazawa, Prog. Part. Nucl. Phys. **90**, 299 (2016) [arXiv:1512.05038].
 - [15] M. Asakawa, U.W. Heinz, and B. Muller, Phys. Rev. Lett. **85**, 2072 (2000) [hep-ph/0003169].
 - [16] B.G. Zakharov, JETP Lett. **63**, 952 (1996) [hep-ph/9607440].
 - [17] B.G. Zakharov, JETP Lett. **65**, 615 (1997) [hep-ph/9704255].
 - [18] B.G. Zakharov, Phys. Atom. Nucl. **61**, 838 (1998) [hep-ph/9807540].
 - [19] T. Anticic *et al.* [NA49 Collaboration], Phys. Rev. C**83**, 014901 (2011) [arXiv:1009.1747].

- [20] M. Anselmino, E. Predazzi, S. Ekelin, S. Fredriksson, and D.B. Lichtenberg, *Rev. Mod. Phys.* **65**, 1199 (1993).
- [21] V.T. Kim, *Mod. Phys. Lett.* **A3**, 909 (1988).
- [22] C. Chen, B. El-Bennich, C.D. Roberts, S.M. Schmidt, J. Segovia, and S. Wan, *Phys. Rev.* **D97**, 034016 (2018) [arXiv:1711.03142].
- [23] N.N. Nikolaev, B.G. Zakharov, and V.R. Zoller, *JETP Lett.* **59**, 6 (1994) [hep-ph/9312268].
- [24] N.N. Nikolaev, G. Piller, and B.G. Zakharov, *J. Exp. Theor. Phys.* **81**, 851 (1995) [hep-ph/9412344].
- [25] Y.V. Kovchegov, A.H. Mueller, *Nucl. Phys.* **B529**, 451 (1998) [hep-ph/9802440].
- [26] R. Baier, Y.L. Dokshitzer, A.H. Mueller, S. Peigné and D. Schiff, *Nucl. Phys.* **B483**, 291 (1997) [hep-ph/9607355].
- [27] B.G. Zakharov, *JETP Lett.* **73**, 49 (2001) [hep-ph/0012360].
- [28] N.N. Nikolaev and B.G. Zakharov, *Phys. Lett.* **B327**, 149 (1994) [hep-ph/9402209].
- [29] Si-xue Qin, Lei Chang, Yu-xin Liu, C.D. Roberts, and D.J. Wilson, *Phys. Rev.* **C84**, 042202 (2011) [arXiv:1108.0603].
- [30] J. Papavassiliou, arXiv:1112.0174.
- [31] A.C. Aguilar, D. Binosi, J. Papavassiliou, and J. Rodriguez-Quintero, *Phys. Rev.* **D80**, 085018 (2009) [arXiv:0906.2633].
- [32] A. Capella and E.G. Ferreira, *Eur. Phys. J.* **C72**, 1936 (2012) [arXiv:1110.6839].
- [33] A. Bialas, M. Bleszynski, and W. Czyz, *Nucl. Phys.* **B111**, 461 (1976).
- [34] D. Kharzeev and M. Nardi, *Phys. Lett.* **B507**, 121 (2001) [nucl-th/0012025].
- [35] G.H. Arakelian, A. Capella, A.B. Kaidalov, and Yu.M. Shabelski, *Eur. Phys. J.* **C26**, 81 (2002) [hep-ph/0103337].
- [36] T. Anticic *et al.* [NA49 Collaboration], *Phys. Rev. Lett.* **93**, 022302 (2004) [nucl-ex/0311024].
- [37] B. Müller and K. Rajagopal, *Eur. Phys. J.* **C43**, 15 (2005) [arXiv:hep-ph/0502174].
- [38] S.V. Afanasiev *et al.* [NA49 Collaboration], *Phys. Rev.* **C66**, 054902 (2002) [nucl-ex/0205002].
- [39] S. Borsanyi, G. Endrodi, Z. Fodor, A. Jakovac, S.D. Katz, S. Krieg, C. Ratti, and K.K. Szabo, *JHEP* **1011**, 077 (2010) [arXiv:1007.2580].
- [40] S.A. Bass, A. Dumitru, M. Bleicher, L. Bravina, E. Zabrodin, H. Stoecker, and W. Greiner, *Phys. Rev.* **C60**, 021902 (1999) [nucl-th/9902062].
- [41] L. Adamczyk *et al.* [STAR Collaboration], *Phys. Rev. Lett.* **112**, 032302 (2014) [arXiv:1309.5681].
- [42] J.L. Albacete, Y.V. Kovchegov, *Nucl. Phys.* **A781**, 122 (2007) [hep-ph/0605053].
- [43] B. Andersson, G. Gustafson, G. Ingelman, and T. Sjostrand, *Phys. Rept.* **97**, 31 (1983).